ACS OMEGA

http://pubs.acs.org/journal/acsodf

Article

Generation of Ultralong Liposome Tubes by Membrane Fusion beneath a Laser-Induced Microbubble on Gold Surfaces

Chiaki Kojima, Akemi Noguchi, Tatsuya Nagai, Ken-ichi Yuyama, Sho Fujii, Kosei Ueno, Nobuaki Oyamada, Kei Murakoshi, Tatsuya Shoji, and Yasuyuki Tsuboi*

Cite This: *ACS Omega* 2022, 7, 13120−13127

Read Online

ACCESS | Metrics & More | Article Recommendations | Supporting Information

ABSTRACT: Membrane fusion (MF) is one of the most important and ubiquitous processes in living organisms. In this study, we developed a novel method for MF of liposomes. Our method is based on laser-induced bubble generation on gold surfaces (a plasmonic nanostructure or a flat film). It is a simple and quick process that takes about 1 min. Upon bubble generation, liposomes not only collect and become trapped but also fuse to form long tubes beneath the bubble. Moreover, during laser irradiation, these long tubes remain stable and move with a waving motion while continuing to grow, resulting in the creation of ultralong tubes with lengths of about 50 μm. It should be noted that the morphology of these ultralong tubes is analogous to that of a sea anemone. The behavior of the tubes was also monitored by fluorescence microscopy. The generation of these ultralong tubes is discussed on the basis of Marangoni convection and thermophoresis.

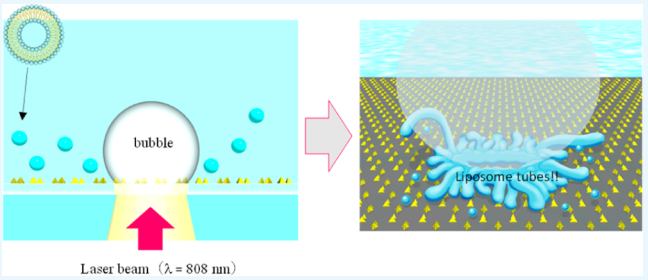

INTRODUCTION

Membrane fusion (MF) is one of the most fundamental, important, and ubiquitous processes in the vital activities of living organisms.[1] MF plays a key role in biological events such as the generation of eukaryotic cells, egg fertilization, cell growth, viral infection, and so on. Therefore, the research on MF has a deep history, and a great deal of effort has been expended in trying to understand the mechanisms underlying MF.[2] Studying membrane fusion in vivo is still a challenging task since it is difficult to predict the timing of the fast cell fusion. Instead, many natural/artificial in vitro systems have recently been studied. Typical target materials are liposomes or vesicles, for which various MF methods have been proposed. In order to understand the fundamental mechanisms of MF, the development of powerful techniques to induce and control MF is clearly indispensable. A representative biochemical approach is reconstitution with SNARE (soluble *N*-ethyl-maleimide-sensitive factor attachment protein receptor) proteins in vitro.[3,4] Also, methods using physical stimuli have been applied. MF techniques using electrical pulses,[5] laser pulses with laser tweezers,[6] plasmonic heating,[7,8] and so forth have been reported so far.

These physical techniques are well-designed and effective for MF. In electric fusion, cells or liposomes/vesicles are collected by electrophoresis to form a pair of particles, and MF is triggered by an irreversible electric breakdown of the membrane at the point of contact of the pair.[5] In the laser method, cells are trapped and manipulated to form a pair at the focal point, and then, the contact area is irradiated by a pulsed laser beam to destroy and fuse the membranes together.[9] In the method using plasmonic heating,[7] a gold nanoparticle, laser-trapped and positioned between a couple of cells or vesicles, is laser-heated to induce MF. All these MF methods consist of two steps. The first step is transportation/manipulation of particles (cells, liposomes, vesicles, etc.) to make contact with each other. The second step is the application of a voltage or laser irradiation to induce MF at the point of contact. It should be noted that Bolognesi et al. recently demonstrated that an optical tweezer is a powerful tool for fusing biomimetic vesicle networks.[10]

There is no doubt that these MF techniques have made great contributions in biological science and cell engineering. On the other hand, both of these two steps require precise operations, and hence, these methods (electrofusion, laser manipulation, plasmonic heating, etc.) are not quick processes, and the production of fused cells and vesicles is limited. Moreover, these laser methods frequently use laser light with high intensity with 200−700 mW laser beams[6−8] focused on the contact area. Such intense laser beam focusing (~MW/cm^2

Received: January 27, 2022
Accepted: March 24, 2022
Published: April 5, 2022

https://doi.org/10.1021/acsomega.2c00553
ACS Omega 2022, 7, 13120−13127

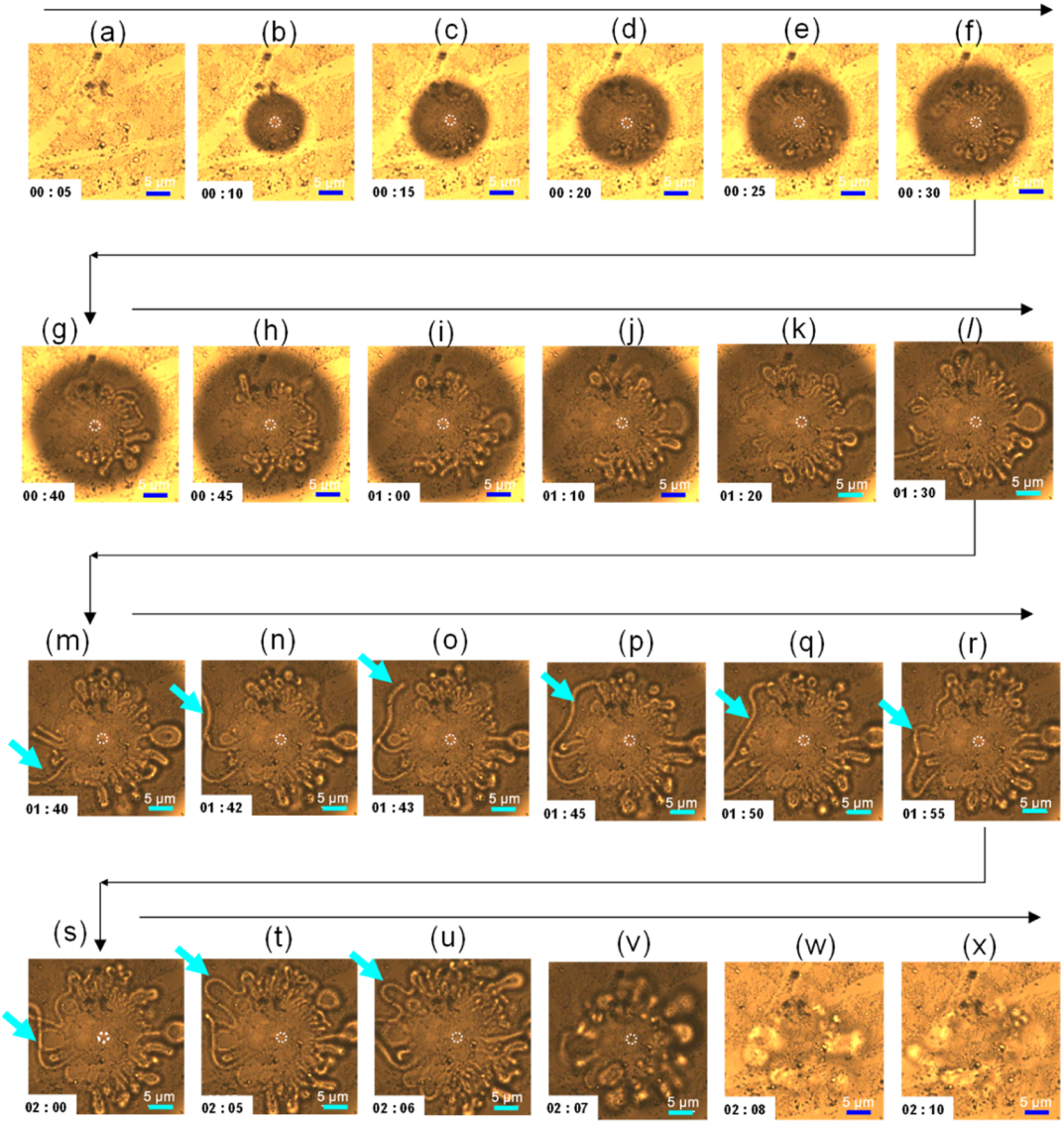

Figure 1. Optical micrographs of ultralong liposome tubes as they develop beneath a laser-induced bubble on a plasmonic nanostructure. The small white circles in the center of each image indicate the laser-irradiated area. Times (min:s) are given in the figure (bottom left of each panel). The laser irradiation (λ = 808 nm, I = 100 kW/cm^2) was started at image (a) and stopped at image (u). The 808 nm irradiation time is (a) 0 min, (b) 5 s, (c) 10 s, (d) 15 s, (e) 20 s, (f) 25 s, (g) 35 s, (h) 40 s, (i) 55 s, (j) 1 min and 5 s, (k) 1 min and 15 s, (l) 1 min and 25 s, (m) 1 min and 35 s, (n) 1 min and 37 s, (o) 1 min and 38 s, (p) 1 min and 40 s, (q) 1 min and 45 s, (r) 1 min and 50 s, (s) 1 min and 55 s, (t) 2 min, and (u) 2 min and 1 s. (v–x) Irradiation was stopped. Scale: bar = 5 μm.

at the focus) is not favorable for maintaining the bio-activity of the cells to be fused. Furthermore, the use of these method has been limited to MF between just two cells. To further develop biological science and cell engineering, it is desirable to have a new technique that enables us to readily and rapidly induce MF among multiple cells.

Here, we demonstrate such a technique for MF, which is based on thermo-plasmonic bubble lithography (TPBL). TPBL, which is analogous to bubble-pen lithography (BL), can manipulate and deposit colloidal nanoparticles on a solid surface with high accuracy, as Lin et al. and other groups have demonstrated in the last few years.[11,12] It should be noted that Iida and his co-workers demonstrated that using a related technique (bubble-pen lithography), a large amount of bacteria (*Escherichia coli*) can be collected while maintaining the bio-activity.[13,14] Also, we succeeded in trapping and fixing living cyanobacteria on a plasmonic nanostructure by means of TPBL.[15] These studies mean that TPBL and bubble-pen lithography are appropriate for living cells and bacteria. In the present study, we applied TPBL to liposomes [diameter (d) ~ 150 nm] homogeneously dispersed in water. We succeeded in obtaining rapid MF of the liposomes by trapping them under a laser-induced micro bubble. Strikingly, the MF resulted in transformation of the liposomes into ultralong liposome tubes (ULTs). These ULTs formed a characteristic assembly around the focal spot with a morphology similar to that of a sea anemone. Moreover, when trapped by laser irradiation, the ULTs kept moving and waving in a similar way to a sea anemone. The features of such MF and the mechanism of formation of the moving ULTs are investigated and discussed.

RESULTS

We prepared liposomes from 3-*sn*-phosphatidylcholine (L-α-phosphatidylcholine) using the Bangham method.[16] These

https://doi.org/10.1021/acsomega.2c00553
ACS Omega 2022, 7, 13120−13127

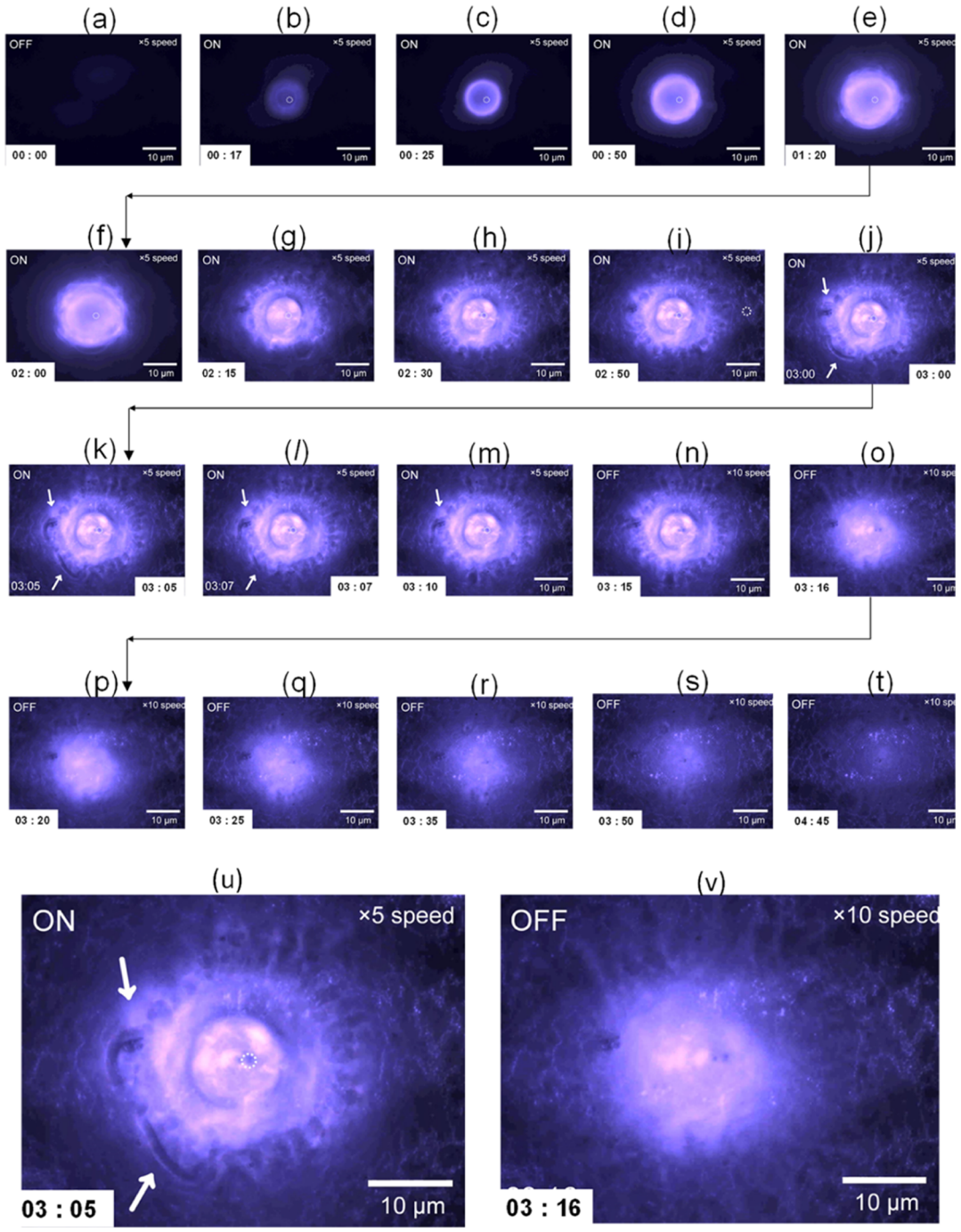

Figure 2. Fluorescence micrographs of ultralong liposome tubes as they develop beneath a laser-induced bubble on a plasmonic nanostructure (corresponding to Figure 1). The small white circles in the center of each image indicate the laser-irradiated area. Times (min:s) are given in the figure (bottom of the left side of each panel). The laser irradiation (λ = 808 nm, I = 100 kW/cm^2) was started at image (b) and stopped around image (n). The irradiation time was (a) 0 s, (b) 2 s, (c) 10 s, (d) 35 s, (e) 1 min and 5 s, (f) 1 min and 45 s, (g) 2 min, (h) 2 min and 15 s, (i) 2 min and 35 s, (j) 2 min and 45 s, (k) 2 min and 50 s, (l) 2 min and 52 s, (m) 2 min and 55 s, and (n) 3 min. (o−t) Irradiation was stopped. Scale: bar = 10 mm. (u) Magnified image of (k). (v) Magnified image of (o).

contain a fluorescent dye (rhodamine B), and the average size (d) was evaluated to be 150 nm. An aqueous solution containing the liposomes was brought into contact with a plasmonic nanostructure comprising a gold nanopyramidal dimer array on a glass cell.[17−19] Our home-made optical tweezers were used to focus a laser onto the sample.[20−22] The sample was irradiated with continuous wave laser light (λ = 808 nm) through an objective lens to resonantly excite gap-mode localized surface plasmons.

When the laser intensity I at the focal point on the plasmonic surface was low (I < 50 kW/cm^2), we did not detect any sign of trapping. When I > 50 kW/cm^2, characteristic and unique trapping behavior was observed. A typical series of optical micrographs (I = 100 kW/cm^2) is displayed in Figure 1, based on which we describe the evolution of the process. Before laser irradiation, the liposomes can scarcely be seen in the sample solution (Figure 1a). This is reasonable since the size of the liposomes used here was 150 nm. When the laser

https://doi.org/10.1021/acsomega.2c00553
ACS Omega 2022, 7, 13120−13127

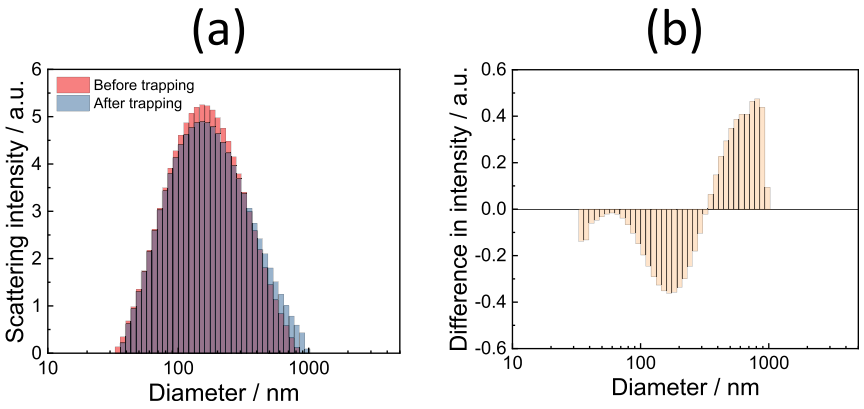

Figure 3. (a) Results of DLS for the sample solution before and after laser irradiation. Laser irradiation was carried out in the following manner. One irradiation cycle consists of 2 min irradiation followed by a 30 s interval without laser irradiation. The DLS was measured after 100 laser irradiation cycles (λ = 808 nm, I = 100 kW/cm^2). (b) Histogram obtained by subtracting these histograms: [histogram (after laser irradiation)] − [histogram (before laser irradiation)].

irradiation is started, a bubble (seen as a dark shadow with a round shape) appears and grows (Figure 1a−i), and about 1 min after starting the irradiation, it reaches a constant size with $d \sim 30$ μm (Figure 1i). This observation is consistent with that in our previous work (TPBL for cyanobacteria).[15] The bubble is generated by the rise in temperature of the water due to a photothermal effect of the plasmonic excitation, which is described in detail later.

As the bubble grows, tube-like objects appear. The tubes increase and grow in length and have a waving motion beneath the bubble (Figure 1c−i). Several long worm-like tubes appear forming a unique and characteristic morphology similar to that of a sea anemone (Figure 1i−u). These long tubes keep moving and waving as if they are alive. It should be pointed out that one of the tubes reached 30 μm in length (marked in Figure 1m−u by the blue arrows). As highlighted in the figure, the growth of these ultralong tubes was observed in real time and represents a new discovery. No such tubes were observed around the center of the bubble. When the laser irradiation was switched off, the bubble vanished, and these ultralong/long tubes were dissipated in the water. In some cases, a bubble remained on the surface even after switching off the laser irradiation. On the other hand, these tubes were transported to the outer sides and partly did not vanish. We observed such a long tube in the solution even 1 h after the stop of laser irradiation, as an optical micrograph is shown in the Supporting Information. Other tubes partly turned into giant-vesicle-like particles. The appearance, growth, and fluctuating motion of these ultralong tubes similar to those of the tentacles of a sea anemone can be observed more clearly in the video movies available in the Supporting Information.

The phenomenon was also monitored by fluorescence microscopy, as shown in Figure 2. The movie of the fluorescence imaging is available in the Supporting Information. Each liposome included a fluorescence dye (rhodamine B) within itself. The advantage of fluorescence imaging is to visualize invisible liposomes and ultralong tubes. Also, density of the concentration of these can be deduced from fluorescence intensity. As clearly realized from the fluorescence images in Figure 2, the sea anemone-like morphology was observed (Figure 2g−n) here also. Following the laser irradiation, the fluorescence spot was observed with a circle shape corresponding to the microbubble (Figure 2b−e). This means that numerous liposomes were collected beneath the bubble. Then, the liposome assembly gradually formed the sea anemone-like morphology (Figure 2f−n). In particular, ultralong tubes were clearly detected as marked by arrows in Figure 2j−m. In Figure 2u, a magnified image of (k) is shown. After the stop of laser irradiation, the fluorescence spot gradually faded away. This means that a part of liposomes assembled beneath the bubble weakly adsorbed on the surface. What is important here is that the ultralong tubes forming the sea anemone-like morphology emitted fluorescence. This indicates that the MF took place rapidly without releasing the dye. Moreover, a random-coil-like network morphology still remained on the gold film even after the stop of laser irradiation (Figure 2n−t). For example, in Figure 2v, a magnified image of Figure 2o is shown. The random-coil-like network morphology is observed surrounding a fluorescence spot where a bubble was generated. We consider that the numerous ultralong tubes adsorbed on the gold film resulted in the network morphology.

Thus, the behavior of the fluorescence (Figure 2) is totally consistent with the bright field observations (Figure 1). Such behavior was observed with 60 < I < 200 kW/cm^2 with good reproducibility.

We examined that whether such ultralong tubes persist after stopping the laser irradiation. Figure 3 shows the results of dynamic light scattering (DLS) of the sample solution, which gave the size distribution of the particles in the solution, before and after laser irradiation (laser irradiation repeated 100 times for 2 min such as shown in Figure 1). There is a slight difference between the histograms before and after laser irradiation. Subtraction of the histograms makes the difference clear. In the sample solution after irradiation, while the number of original liposomes ($d \sim 150$ nm) decreased, large particles ($d \sim 1000$ nm) appeared. The result obviously means that the larger particles seen in Figure 1 still remain in the solution even after stopping the laser irradiation. The reason why the difference in DLS was slight is noted as follows. The ratio of total irradiated volume of the solution that interacted with the bubble to the total solution volume (50 μL) was much small. We tried to make the difference obvious by increasing the number of laser irradiation events (over 300 times irradiation events). However, the difference was still small.

We also investigated traditional optical trapping of the liposomes (without using the plasmonic substrate) and optical trapping with a nanostructured Si crystal (black silicon) in

https://doi.org/10.1021/acsomega.2c00553
ACS Omega 2022, 7, 13120−13127

place of the plasmonic nanostructure.[23] The results are shown in the Supporting Information. This shows that trapping of liposomes occurred, but such ultralong tube formation was not observed. This indicates that the formation of the ultralong tubes was triggered not by the optical gradient force but by thermal effects. Therefore, before discussing the detailed mechanism underlying the tubulation, we measured the thermal features of the system. We measured the temperature distribution around the irradiation area using a water-soluble fluorescence probe whose fluorescence intensity was very sensitive to temperature.[24] Because it was difficult to measure the temperature beneath the bubble, we measured the temperature (T) during laser irradiation at an intensity (I) marginal to the threshold for bubble generation (I_{th} > 50 kW/cm^2). In Figure 4, the rise in temperature (ΔT) is plotted

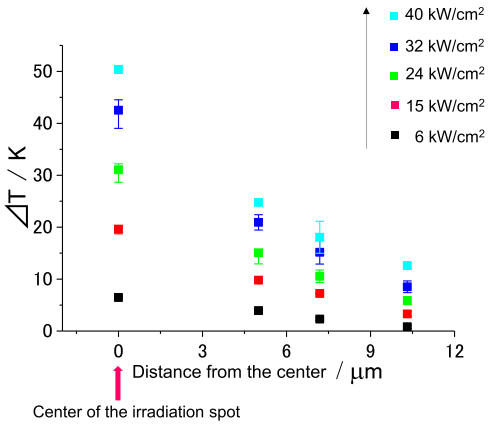

Figure 4. Spatial profile of the rise in temperature (DT) on the plasmonic surface as a function of laser intensity. The distance from the center of the irradiation spot is indicated on the abscissa. The laser intensity is given in the figure. The slope of each dependence corresponds to the temperature gradient (dT/dr).

against the position (r; distance from the irradiation focus) as a function of I. When I = 40 kW/cm^2, ΔT was 50 K meaning that T = 73 °C at the center of the irradiation area at a room temperature of 23 °C. With increasing r, T decreases steeply with a temperature gradient of dT/dr = 3.5 K/μm. This means that a huge temperature gradient was generated around the irradiation area. It should be pointed out that the temperature gradient (slope of the plot in Figure 4) increases with increasing I, indicating that a larger temperature gradient than 3.5 K/μm was generated in the case shown in Figure 1 (I = 100 kW/cm^2). It is assumed that these thermal features are involved in the formation of the ultralong tube assemblies, the details of which are discussed in the following.

As a control experiment, we investigated BL using a flat thin gold film deposited on a cover slip. Because of the lack of a nanostructure (nano-gaps), there should only be a photothermal effect with this substrate. Also, in this case, a micro bubble appeared on the gold film under laser irradiation (λ = 808 nm, I = 100 kW/cm^2), as other researchers have already reported. Following the bubble formation, also in this case, a similar phenomenon of the ultralong tube generation was generated. The sea anemone-like morphology and moving/waving were observed. Such behavior is displayed in Figure 5. This clearly means that the phenomenon was triggered and induced not by a plasmon-enhanced optical force but by photothermal effects. The mechanism underlying the MF leading to the ultralong tube generation is discussed in the next section.

DISCUSSION

Clearly, the ultralong tubes are made of liposomes (ULTs). As shown in the DLS measurements, these ULTs were stably maintained even after stopping the laser irradiation. This means that the ultralong tubes are produced by MF of the liposomes. This is consistent with the observation that no interface (between liposome particles) was observed in any of the long tubes. Each liposome included a fluorescence dye (rhodamine B) within itself. This indicates that the MF took place rapidly without releasing the dye. To understand the overall mechanism underlying the phenomenon, we should discuss three processes: membrane fusion, tubulation, and the waving motion. In BL, the fluid (water) surrounding the bubble should behave as shown by the illustrations in Figure 6.

Around the bubble, Marangoni convection occurs. Near the surface of the substrate, the convection is directed from the outer side to the center of the bubble.[11,12,25] Namura et al. reported that such Marangoni convection should generate mechanical force parallel to a substrate surface with a magnitude of <1 mN.[25] Accordingly, the liposomes should collect at the bottom of the bubble (in the narrow space between the bubble surface and the plasmonic substrate) and be subjected to a high pressure. It was recently reported that high pressure frequently induced MF of vesicles.[26] We consider the high pressure near the center of the bottom of the bubble to be the origin of the MF. With such MF, giant liposomes should be generated. As shown in Figure 4, the temperature at the center of the bottom of the bubble is raised by ΔT > 50 K. Also, for the gold flat film, ΔT was evaluated to be ΔT > 50 K.

On the other hand, it is well known that the deformation of vesicles and liposomes is induced by dehydration. Characteristic morphologies and shapes of vesicles and liposomes by such deformation due to dehydration have been reported. In the present case, it is assumed that the giant liposomes generated by MF beneath the bubble become dehydrated due to the high pressure and high temperature. Presumably, this is the origin of the ULTs. It is well known that liposomes consisting of phosphatidylcholine exhibit gel−liquid crystal phase transition around $T \sim 50$ °C. The present temperature $T \geq 70$ °C (corresponding to ΔT > 50 K) is higher than the phase transition temperature. Therefore, we deduce the mechanism of MF: The lipid membrane of liposomes beneath the microbubble should undergo the phase transition to increase membrane fluidity, leading to MF among adjacent liposomes.

These tubes continually wave and fluctuate during laser irradiation. In addition to Marangoni convection, another force is exerted on the ultralong liposome tubes beneath the bubble. This is a thermophoretic force due to the huge temperature gradient of dT/dr > 3.5 K/μm (Figure 4). For the flat gold film, the temperature gradient was evaluated to be $dT/dr \sim 3$ K/μm. The gradient is much larger than the typical values reported for thermophoresis of colloidal particles (dT/dr < 1 K/μm).[27] The thermophoretic force (F_T) is proportional to the temperature gradient[24]

$$F_T = -S_T k_B T \nabla T \quad (1)$$

where S_T is the Soret coefficient, k_B is the Boltzmann constant, T is the temperature, and ∇T (=dT/dr) is the temperature

https://doi.org/10.1021/acsomega.2c00553
ACS Omega 2022, 7, 13120−13127

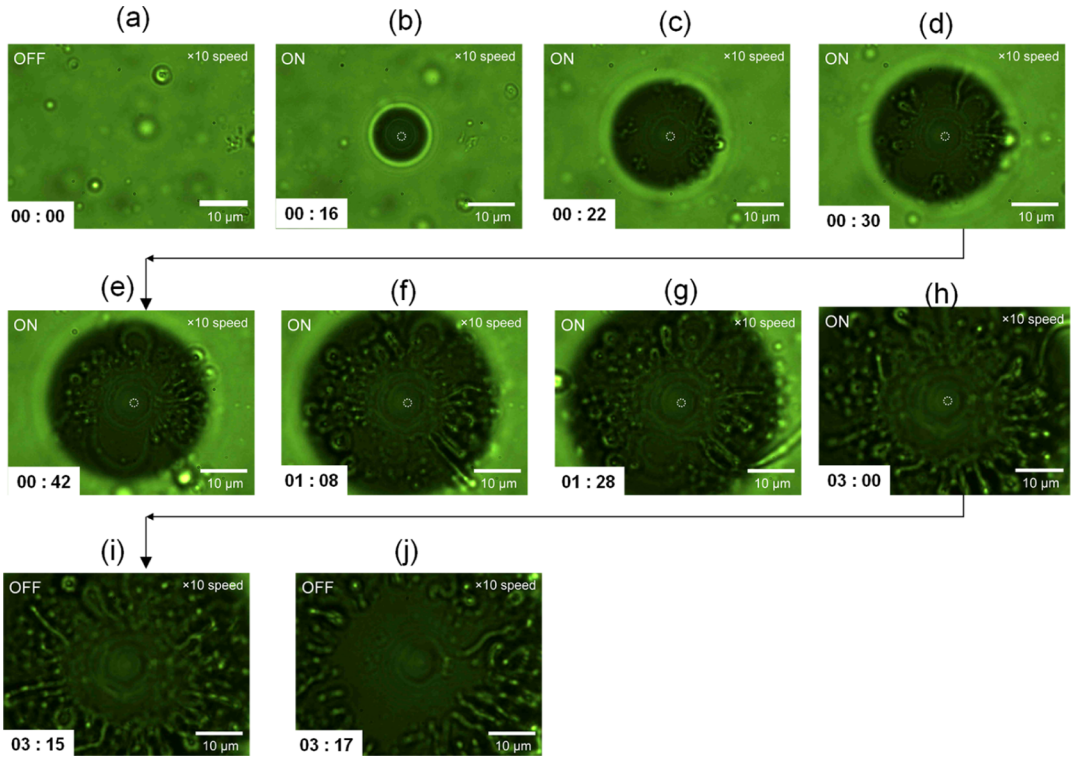

Figure 5. Optical micrographs of ultralong liposome tubes as they develop beneath a laser-induced bubble on a flat gold film. The small white circles in the center of each image indicate the laser-irradiated area. Times (min:s) are given in the figure (bottom left of each panel). The laser irradiation (λ = 808 nm, I = 100 kW/cm^2) was started around (b) and stopped at image (i). Irradiation time was (a) 0 s, (b) 1 s, (c) 7 s, (d) 15 s, (e) 37 s, (f) 53 s, (g) 1 min and 13 s, (h) 2 min and 45 s, and (i) 3 min. (j) Irradiation was stopped. Scale: bar = 10 μm.

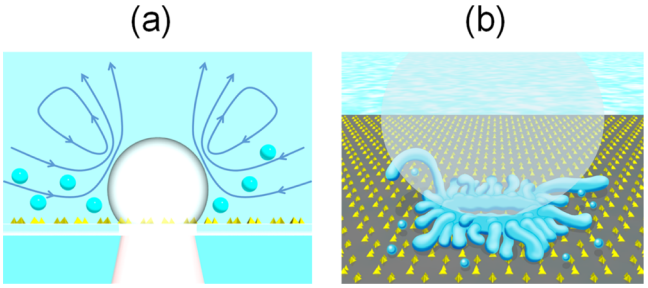

Figure 6. (a) Schematic illustration of laser-induced bubble formation on the plasmonic nanostructure followed by liposome trapping. The direction of Marangoni convection is also indicated on the basis of refs 11 and 25. Adapted with permission from Lin, L., Peng, X., Mao, Z., Li, W., Yogeesh, M. N., Rajeeva, B. B., Perillo, E. P., Dunn, A. K., Akinwande, D. and Zheng, Y. Bubble-Pen Lithography. *Nano Lett.* **2016,** *16,* 701−708. Copyright 2016 of the American Chemical Society. (b) Schematic illustration of the generation of ULTs.

gradient. Adopting the value of S_T = 0.3 K^{-1},[28] F_T is 5.0 fN. This force plays a part in a driving the waving motion. The thermophoresis transports the liposomes from the hotter region to the colder region beneath the bubble. These forces, due to Marangoni convection and thermophoresis, result in the waving motion of ultralong tubes. Moreover, Kudella et al. reported that the temperature gradient can deform liposomes above phase transition temperature.[29] Such an effect should be involved in the ultralong tube generation.

In summary, we discovered rapid MF of liposomes in TPBL. This is a simple, rapid, and convenient method to produce giant liposomes via MF. What is important here is that the MF is accompanied by tubulation, producing ULTs. Because these tubes partly remained stable and still retained the rhodamine dye within them even after switching off the laser irradiation, it was obvious that these tubes were produced by MF. Other tubes seemed to change to giant vesicles with a spherical shape. Such rapid and efficient MF was induced by the high temperature and high pressure beneath the bubble. Moreover, the waving motion of these ultralong tubes was maintained during irradiation. The driving force of the waving motion is presumably Marangoni convection and the thermophoretic force. The phenomenon and the method are applicable to research in MF, cell engineering, and general vesicle science. Moreover, we have demonstrated that bubble generation can promote MF.

METHODS

3-*sn*-Phosphatidylcholine (L-α-phosphatidylcholine) was purchased from FUJIFILM Wako Pure Chemical Co. Ltd. and used without further purification. This, together with rhodamine B, was dissolved in chloroform and dried. Then, the residue was dissolved in pure water (Milli-Q) using a supersonic homogenizer (As One, Sonicstar 85). The solution was dialyzed to eliminate excess rhodamine B. The size of the liposomes was evaluated using DLS (Otsuka Electronics Co., Ltd.). The plasmonic glass substrate, on which the gold nanopyramidal dimer arrays were integrated, was fabricated by means of angle-resolved nanosphere lithography. Gold was vacuum deposited on a glass substrate to form a thin film (thickness ∼ 10 nm). The plasmonic nanostructure was brought into contact with the sample solution in a glass cell. Details of our optical tweezers have already been reported and are briefly described here.[15] We used a cw near-infrared (λ = 808 nm) diode laser (Shanghai Laser & Optics Century Co.,

https://doi.org/10.1021/acsomega.2c00553
ACS Omega 2022, 7, 13120−13127

Ltd., IRM808TA-200SR) for resonant excitation of gap-mode plasmons on the gold nanopyramidal dimer arrays. UV light from a Hg lamp was used for fluorescence excitation. The laser beam and UV light were co-axially introduced into a confocal optical microscope and focused onto the sample cell. The trapping behavior was analyzed by observations made with the microscope.

■ ASSOCIATED CONTENT

Supporting Information

The Supporting Information is available free of charge at https://pubs.acs.org/doi/10.1021/acsomega.2c00553.

Movie of ultralong tube generation (MP4)

Long-lived long tube after the stop of laser irradiation and fluorescence micrographs of trapping behavior of liposomes (PDF)

Optical trapping behavior of liposomes on nano-structured Si (black Si) (MP4)

■ AUTHOR INFORMATION

Corresponding Author

Yasuyuki Tsuboi − *Division of Molecular Materials Science, Graduate School of Science, Osaka City University, Sumiyoshi, Osaka 558-8585, Japan;* orcid.org/0000-0002-1057-939X; Email: twoboys@sci.osaka-cu.ac.jp

Authors

Chiaki Kojima − *Division of Molecular Materials Science, Graduate School of Science, Osaka City University, Sumiyoshi, Osaka 558-8585, Japan*

Akemi Noguchi − *Division of Molecular Materials Science, Graduate School of Science, Osaka City University, Sumiyoshi, Osaka 558-8585, Japan*

Tatsuya Nagai − *Division of Molecular Materials Science, Graduate School of Science, Osaka City University, Sumiyoshi, Osaka 558-8585, Japan*

Ken-ichi Yuyama − *Division of Molecular Materials Science, Graduate School of Science, Osaka City University, Sumiyoshi, Osaka 558-8585, Japan;* orcid.org/0000-0002-6998-6942

Sho Fujii − *Graduate School of Chemical Sciences and Engineering, Hokkaido University, Sapporo, Hokkaido 060-0808, Japan; National Institute of Technology, Kisarazu College, Kisarazu City 292-0041 Chiba, Japan;* orcid.org/0000-0002-6774-1482

Kosei Ueno − *Graduate School of Chemical Sciences and Engineering, Hokkaido University, Sapporo, Hokkaido 060-0808, Japan;* orcid.org/0000-0002-4882-7854

Nobuaki Oyamada − *Graduate School of Chemical Sciences and Engineering, Hokkaido University, Sapporo, Hokkaido 060-0808, Japan;* orcid.org/0000-0002-4241-6851

Kei Murakoshi − *Graduate School of Chemical Sciences and Engineering, Hokkaido University, Sapporo, Hokkaido 060-0808, Japan;* orcid.org/0000-0003-4786-0115

Tatsuya Shoji − *Department of Chemistry, Faculty of Science, Kanagawa University, Hiratsuka 259-1293, Japan;* orcid.org/0000-0001-7213-6466

Complete contact information is available at: https://pubs.acs.org/10.1021/acsomega.2c00553

Notes

The authors declare no competing financial interest.

■ ACKNOWLEDGMENTS

The authors in Japan are grateful for the financial support of JSPS KAKENHI grant numbers JP17K04974, JP18K14254, JP19H02737, JP20H02550, JP21K04744, and JP16H06506/JP16H06507 in Scientific Research on Innovative Areas "Nano-Material Manipulation and Structural Order Control with Optical Forces" and "Molecular Engine" (JP19H05402). Also, the authors are grateful for the financial support from the SEI (Sumitomo Electric Industry) Group Foundation and the CANON Foundation. The authors are grateful to prof. Makoto Miyata (Osaka City Univ.) for his helpful discussion.

■ REFERENCES

(1) Singer, S. J.; Nicolson, G. L. The Fluid Mosaic Model of the Structure of Cell Membranes. *Science* **1972**, *175*, 720−731.

(2) Blumenthal, R.; Clague, M. J.; Durell, S. R.; Epand, R. M. Membrane Fusion. *Chem. Rev.* **2003**, *103*, 53−70.

(3) Jahn, R.; Scheller, R. H. SNAREs — engines for membrane fusion. *Nat. Rev. Mol. Cell Biol.* **2006**, *7*, 631−643.

(4) Lira, R. B.; Robinson, T.; Dimova, R.; Riske, K. A. Highly Efficient Protein-free Membrane Fusion: A Giant Vesicle Study. *Biophys. J.* **2019**, *116*, 79−91.

(5) Stoicheva, N. G.; Hui, S. W. Electrofusion of cell-size liposomes. *Biochim. Biophys. Acta Biomembr.* **1994**, *1195*, 31−38.

(6) Steubing, R. W.; Cheng, S.; Wright, W. H.; Numajiri, Y.; Berns, M. W. Laser induced cell fusion in combination with optical tweezers: The laser cell fusion trap. *Cytometry* **1991**, *12*, 505−510.

(7) Rørvig-Lund, A.; Bahadori, A.; Semsey, S.; Bendix, P. M.; Oddershede, L. B. Vesicle Fusion Triggered by Optically Heated Gold Nanoparticles. *Nano Lett.* **2015**, *15*, 4183−4188.

(8) Hill, E. H.; Li, J.; Lin, L.; Liu, Y.; Zheng, Y. Opto-Thermophoretic Attraction, Trapping, and Dynamic Manipulation of Lipid Vesicles. *Langmuir* **2018**, *34*, 13252−13262.

(9) Techaumnat, B.; Washizu, M. Analysis of the effects of an orifice plate on the membrane potential in electroporation and electrofusion of cells. *J. Phys. D. Appl. Phys.* **2007**, *40*, 1831−1837.

(10) Bolognesi, G.; Friddin, M. S.; Salehi-Reyhani, A.; Barlow, N. E.; Brooks, N. J.; Ces, O.; Elani, Y. Sculpting and fusing biomimetic vesicle networks using optical tweezers. *Nat. Commun.* **2018**, *9*, 1882.

(11) Lin, L.; Peng, X.; Mao, Z.; Li, W.; Yogeesh, M. N.; Rajeeva, B. B.; Perillo, E. P.; Dunn, A. K.; Akinwande, D.; Zheng, Y. Bubble-Pen Lithography. *Nano Lett.* **2016**, *16*, 701−708.

(12) Fujii, S.; Kanaizuka, K.; Toyabe, S.; Kobayashi, K.; Muneyuki, E.; Haga, M.-a. Fabrication and Placement of a Ring Structure of Nanoparticles by a Laser-Induced Micronanobubble on a Gold Surface. *Langmuir* **2011**, *27*, 8605−8610.

(13) Yamamoto, Y.; Shimizu, E.; Nishimura, Y.; Iida, T.; Tokonami, S. Development of a rapid bacterial counting method based on photothermal assembling. *Opt. Mater. Express* **2016**, *6*, 1280−1285.

(14) Tokonami, S.; Kurita, S.; Yoshikawa, R.; Sakurai, K.; Suehiro, T.; Yamamoto, Y.; Tamura, M.; Karthaus, O.; Iida, T. Light-induced assembly of living bacteria with honeycomb substrate. *Sci. Adv.* **2020**, *6*. DOI: 10.1126/sciadv.aaz5757.

(15) Naka, S.; Shoji, T.; Fujii, S.; Ueno, K.; Wakisaka, Y.; Murakoshi, K.; Mizoguchi, T.; Tamiaki, H.; Tsuboi, Y. Thermo-Plasmonic Trapping of Living Cyanobacteria on a Gold Nanopyramidal Dimer Array: Implications for Plasmonic Biochips. *ACS Appl. Nano Mater.* **2020**, *3*, 10067−10072.

(16) Uda, R. M.; Hiraishi, E.; Ohnishi, R.; Nakahara, Y.; Kimura, K. Morphological Changes in Vesicles and Release of an Encapsulated Compound Triggered by a Photoresponsive Malachite Green Leuconitrile Derivative. *Langmuir* **2010**, *26*, 5444−5450.

(17) Suzuki, K.; Li, X.; Wang, Y.; Nagasawa, F.; Murakoshi, K. Active Intermediates in Plasmon-Induced Water Oxidation at Au Nanodimer Structures on a Single Crystal of TiO2. *ACS Energy Lett.* **2020**, *5*, 1252−1259.

(18) Zhang, J.; Zhou, R.; Minamimoto, H.; Yasuda, S.; Murakoshi, K. Nonzero Wavevector Excitation of Graphene by Localized Surface Plasmons. *Nano Lett.* **2019**, *19*, 7887−7894.
(19) Takase, M.; Ajiki, H.; Mizumoto, Y.; Komeda, K.; Nara, M.; Nabika, H.; Yasuda, S.; Ishihara, H.; Murakoshi, K. Selection-rule breakdown in plasmon-induced electronic excitation of an isolated single-walled carbon nanotube. *Nat. Photonics* **2013**, *7*, 550−554.
(20) Tsuboi, Y.; Shoji, T.; Kitamura, N.; Takase, M.; Murakoshi, K.; Mizumoto, Y.; Ishihara, H. Optical Trapping of Quantum Dots Based on Gap-Mode-Excitation of Localized Surface Plasmon. *J. Phys. Chem. Lett.* **2010**, *1*, 2327−2333.
(21) Shoji, T.; Saitoh, J.; Kitamura, N.; Nagasawa, F.; Murakoshi, K.; Yamauchi, H.; Ito, S.; Miyasaka, H.; Ishihara, H.; Tsuboi, Y. Permanent Fixing or Reversible Trapping and Release of DNA Micropatterns on a Gold Nanostructure Using Continuous-Wave or Femtosecond-Pulsed Near-Infrared Laser Light. *J. Am. Chem. Soc.* **2013**, *135*, 6643−6648.
(22) Hashimoto, S.; Uenobo, Y.; Takao, R.; Yuyama, K.-i.; Shoji, T.; Linklater, D. P.; Ivanova, E.; Juodkazis, S.; Kameyama, T.; Torimoto, T.; Tsuboi, Y. Incoherent Optical Tweezers on Black Titanium. *ACS Appl. Mater. Interfaces* **2021**, *13*, 27586−27593.
(23) Komoto, S.; Nagai, T.; Takao, R.; Ushiro, K.; Matsumoto, M.; Shoji, T.; Linklater, D. P.; Juodkazis, S.; Tsuboi, Y. Optical Trapping of Polystyrene Nanoparticles on Black Silicon: Implications for Trapping and Studying Bacteria and Viruses. *ACS Appl. Nano Mater.* **2020**, *3*, 9831−9841.
(24) Shoji, T.; Itoh, K.; Saitoh, J.; Kitamura, N.; Yoshii, T.; Murakoshi, K.; Yamada, Y.; Yokoyama, T.; Ishihara, H.; Tsuboi, Y. Plasmonic Manipulation of DNA using a Combination of Optical and Thermophoretic Forces: Separation of Different-Sized DNA from Mixture Solution. *Sci. Rep.* **2020**, *10*, 3349.
(25) Namura, K.; Imafuku, S.; Kumar, S.; Nakajima, K.; Sakakura, M.; Suzuki, M. Direction control of quasi-stokeslet induced by thermoplasmonic heating of a water vapor microbubble. *Sci. Rep.* **2019**, *9*, 4770.
(26) Goto, M.; Kazama, A.; Fukuhara, K.; Sato, H.; Tamai, N.; Ito, H.-O.; Matsuki, H. Membrane fusion of phospholipid bilayers under high pressure: Spherical and irreversible growth of giant vesicles. *Biophys. Chem.* **2021**, *277*, 106639.
(27) Kołacz, J.; Konya, A.; Selinger, R. L. B.; Wei, Q. H. Thermophoresis of colloids in nematic liquid crystal. *Soft Matter* **2020**, *16*, 1989−1995.
(28) Talbot, E. L.; Kotar, J.; Parolini, L.; Di Michele, L.; Cicuta, P. Thermophoretic migration of vesicles depends on mean temperature and head group chemistry. *Nat. Commun.* **2017**, *8*, 15351.
(29) Kudella, P. W.; Preißinger, K.; Morasch, M.; Dirscherl, C. F.; Braun, D.; Wixforth, A.; Westerhausen, C. Fission of Lipid-Vesicles by Membrane Phase Transitions in Thermal Convection. *Sci. Rep.* **2019**, *9*, 18808.

https://doi.org/10.1021/acsomega.2c00553
ACS Omega 2022, 7, 13120−13127